J. Phys. D: Appl. Phys. **43** (2010) 035103 (7pp) doi:10.1088/0022-3727/43/3/035103

Rubbing effects on the structural and optical properties of poly(3-hexylthiophene) films

M Abbas[1], F D'Amico[2], M Ali[1], I Mencarelli[3], L Setti[3], E Bontempi[4], R Gunnella[1,5]

[1] CNISM-Università di Camerino, Via Madonna delle Carceri, 62032 Camerino (MC), Italy
[2] Sincrotrone Trieste S.C.p.A., Strada Statale 14-Km 163.5 in Area Science Park, 34012 Basovizza, Trieste, Italy
[3] Department of Industrial and Materials Chemistry, University of Bologna, V. Risorgimento 4, 40136 Bologna, Italy
[4] Chemistry for Technologies Laboratory, University of Brescia, via Branze 38, 25123, Brescia, Italy

E-mail: roberto.gunnella@unicam.it

Received 8 June 2009, in final form 27 November 2009
Published 8 January 2010
Online at stacks.iop.org/JPhysD/43/035103

Abstract
Steady state photoconductivity and x-ray diffraction combined with optical and electronic spectroscopies were applied to study spin coated poly(3-hexylthiophene) (P3HT) films mechanically rubbed using a teflon bar. As expected, photoconductivity evidenced a strong increase in the photo-response along the rubbing direction. But, while rubbing during annealing at a temperature of 70 °C resulted in a sizeable photocurrent anisotropy along the direction parallel or perpendicular to the rubbing, the samples rubbed at room temperature (RT) showed an isotropic and comparatively stronger enhancement of absorption and photoconductivity spectral features. According to these observations, rubbing at RT resulted in a significant increase in local order and macroscopic alignment of the film, while a higher degree of global order but with a relaxed local structure was obtained after rubbing at 70 °C.

1. Introduction

Regio-regular poly(3-hexylthiophene) (P3HT) was the first polymeric semiconductor to show sizeable carrier mobility above 0.1 $cm^2 V^{-1}s^{-1}$ [1, 2]. Nowadays, it remains one of the most promising materials for applications in organic field effect transistors, thin-film transistors [3] and organic photovoltaic cells [4, 5]. Polythiophene films grown at room temperature (RT) by casting or spin coating have the peculiarity of self-assembling into crystallites, a few tens of nanometres in size, separated by amorphous materials [6]. As in other conjugated polymers, one-dimensional semiconducting properties of P3HT are provided by the unhybridized carbon p_z orbital along the polymer backbone. Nevertheless, the microstructure of the film plays a key role in controlling charge hopping processes between two adjacent chains, leading to a two-dimensional carrier mobility, while in the remaining third direction such a mobility is limited by the insulating alkyl chains.

Depending on the molecular weight, the growth conditions (drop casting versus spin coating) or the solvent boiling point, the P3HT has been observed to develop elongated crystallites [7] even in thin films [8]. In such linear structures, the backbone of the polymer is perpendicular to the main axis. At high molecular weights or fast deposition rates, the reduced dynamics favour the formation of nodular structures or rod-like structures containing folded chains. The width of these structures depends on the molecular weight of the polymer [9, 10]. Conductivity in the plane of the film is related to the 'edge-on' conformation of the polymer chains on the substrate as demonstrated by Sirringhaus *et al* [11]. Such a conductivity was found about three orders of magnitude larger than the conductivity in films with 'plane-on' oriented chains. A similar increase in conductivity is observed with the increase in molecular weight. In this latter case, conductivity is not correlated with the crystallinity of the film, because

[5] Author to whom any correspondence should be addressed.

high molecular weight films show lower crystallinity [9]. A possible explanation is related to the poor conductivity at the boundaries between structures when they are made by low molecular weight P3HT (fibrils) while a better connectivity is obtained by high molecular weight P3HT. Further evidence is the optical absorption spectra with red shift observed in high molecular weight films and the formation of clear vibronic structures due to planar configuration of the chains [12].

To further improve the efficiency of devices based on P3HT, the surface film properties can be properly modified by means of mechanical or electrostatic methods. Different techniques have been proposed to orient the polymer with an expected large economic impact on the industrial processes involved [13, 14].

Mechanical rubbing, though limited to the superficial region of the film, is one of the possible post-growth techniques that can be used to overcome the limitations of the hopping mechanisms in the conduction processes and has been commonly used to control the alignment of the liquid crystals on the polymers [15]. Although the relationship between structural and functional properties of the polymers after the treatment has received considerable attention [16, 17], the physical mechanisms are still to be clarified. Only a few studies have been performed so far to understand the ordering properties after rubbing using either a velvet tissue [18, 19] or a smooth piece of quartz [20]. It is beyond the scope of this study to investigate which one of such rubbing techniques is more suitable and efficient for the alignment of the P3HT films. This study will focus on how the physical/microscopic properties are affected after a particular rubbing mechanism has created a sizeable film anisotropy.

Few examples in the literature are the work of Yang *et al* [20], who put into evidence the anisotropy induced by rubbing on photoconductivity with electric field along the rubbing direction or perpendicular to it, and Heil *et al* [19] who studied the field effect mobility. Rubbing was performed in both cases at about 100 °C to optimize the mobility of the films [21].

In such a scenario, the results we present aim at completing the picture of the structural modifications achieved by rubbing at RT and at temperatures well below the glass transition (70 °C). Several issues deserve proper attention in these kinds of studies: the role of starting microstructure on which rubbing is performed; the possibility that the film is modified during the rubbing; the corresponding modifications which should be observed on both the photo-carrier generation and transport properties after annealing. We find that the modifications induced on the films systematically recorded can shed light on the photo-generation and photoconductive mechanisms in thin films of this important polymer.

2. Experimental section

P3HT films, 200 nm thick, were deposited from $CHCl_3$ (1 mg ml^{-1}) solvent by spin-coating on Corning glass and on SiO_2 substrates. Head-to-tail 92% regio-regularity was determined by ^{1}H nuclear magnetic resonance, while molecular weight (M_w) in excess of 50 kD and poly-dispersity about 2.1 were determined by gel permeation chromatography. The samples were mechanically rubbed in air by a Teflon bar along one particular direction at RT and at 70 °C, respectively. After the preparation, the thin films obtained from a fresh solution turned out to be quite stable if properly preserved in dark and controlled ambient temperature. The morphology of the P3HT film was analysed by atomic force microscopy (AFM) (Veeco 5000 Dimension) working in tapping mode with a cantilever frequency of 270 kHz. AFM quantitative morphological analysis was performed using WSxM software [22]. Both absorption and photoconductivity spectra were obtained by using a lock-in amplifier and an optical chopper. The working frequency chosen was 30 Hz. The absorption measurements were carried out by measuring the normalized transmitted light intensity using a silicon PIN detector.

In order to measure photoconductivity, tin electrodes spaced 500 μm were evaporated over the samples under vacuum (6×10^{-5} Pa) to collect currents in both the parallel ('para') and perpendicular ('ortho') directions with respect to the rubbing orientation. The photoconductive signal was measured over the load resistance (20 MΩ) under an electric field of 1.6×10^3 V cm^{-1}. The incoming light power was derived from the standard photoresponse of the silicon detector to normalize the photo-response spectra of the samples.

Two-dimensional x-ray diffraction (XRD^2) was collected by means of a Rigaku D-Max Rapid diffractometer, equipped with a two-dimensional image-plate detector, using Cu K_α radiation.

In order to check the stability of the polymer we performed x-ray photoelectron spectroscopy (XPS) by using an Al K_α un-monochromatized x-ray source. The investigation of the valence band spectra by means of ultraviolet photoelectron spectroscopy (UPS) was performed on the samples grown on the native oxide of silicon substrates in order to minimize charging effects. UPS spectra were acquired at a pressure of $\sim 10^{-9}$ Torr using a He discharge lamp providing He I (21.2 eV) and He II (40.8 eV) lines impinging at 45° with respect to the detection direction of an hemispherical electron analyzer VG-CLAM4.

3. Results

3.1. Microscopy

In figure 1 we report the images of the pristine samples, before (*a*) and after the modifications induced by rubbing at RT (*b*) and at 70 °C (*c*). Strong modifications of the surface were observed from the nodular isotropic morphology by the application of mechanical alignment along the direction of scanning (left to right). Modifications in the morphology were accompanied by the increase in the roughness from 0.2 to 0.3 nm of the pristine samples (figure 1(*a*), in good agreement with previous measurements [9]) to a much larger one (1.5–2.0 nm) in the latter two cases of figures 1(*b*) and (*c*).

But, while the RT rubbed samples did not show any modification in the common nodular structure, if we exclude a slight orientation along the rubbing direction observed in figure 1(*b*), the 70 °C rubbed samples underwent a structural transition leading to the formation of meander-like rods of

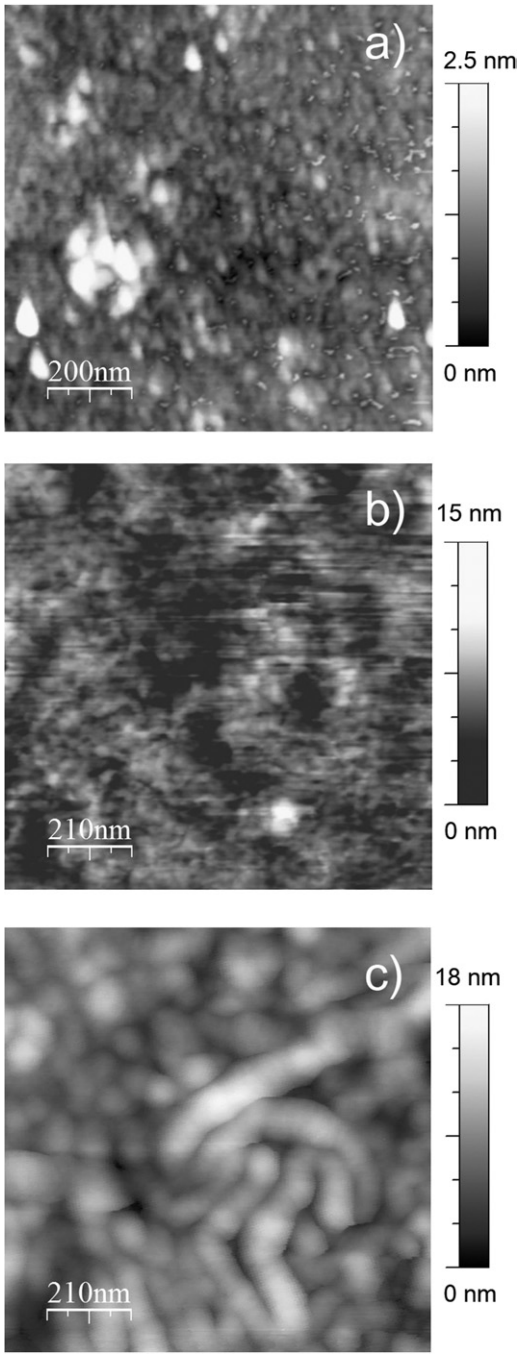

Figure 1. AFM images of pristine (*a*) (roughness (r) = 0.38 nm), RT rubbed (*b*) (r = 1.19 nm) and 70 °C rubbed (*c*) (r = 2.37 nm). Direction of the rubbing is left to right.

dimension 100 nm, ten times larger than the rods usually observed in the low M_w P3HT films [9].

3.2. X-ray diffraction

In order to provide a quantitative determination of the P3HT films surface structure and its modifications induced by rubbing, we performed XRD^2 in grazing incidence. XRD^2 is extremely useful to determine the surface structure in those systems whose physical properties of interest are confined at the interface region or where modifications have taken place. With this aim, we used a Cu K_α source and two measurement modes, hereafter named 'grazing' and 'rotating' mode. In the former case, a grazing incidence geometry at about 1° was used. In the latter case, the samples were continuously rotated around the incidence angle by a few degrees in the polar and azimuthal directions.

The diffraction features recorded are the (h 0 0)-reflection peaks at about $2\theta = 5°$ and 10°, corresponding, within the unit cell model proposed by Prosa *et al* [23], to the inter-layer alkyl chains in the lamellar structure (a = 16.8 Å, $q = 2\pi/d$ = 0.37 Å^{-1}). A second feature labelled (0 1 0) at $\theta = 23.4°$, corresponding to $q = 2\pi/d$ = 1.65 Å^{-1}, is due to the inter-layer distance ($b/2$ = 3.8 Å) of the π–π stacking [23].

In high regio-regularity P3HT, a predominance of molecules whose thiophene rings with 'edge-on' orientation and stacking direction ([0 1 0]) parallel to the surface was reported, while the axes of the [1 0 0] alkyl chains were perpendicular to the surface [11]. In this regard, we checked the presence of polymer configurations with planar rings ('plane-on') as observed in low regio-regularity P3HT films measured by specular diffraction. No intensity in transmission XRD and out-of-plane scattering geometry was found with the exception of the (1 0 0) peak.

In figure 2 we report from (*a*) to (*c*) the XRD^2 patterns for a grazing angle of 1° for the pristine, RT rubbed and 70 °C rubbed samples, respectively. Although the incidence angle of 1° was above the critical angle, we took advantage of the good signal-to-noise ratio obtained from the film in this configuration with a reduced background from the substrate. It is clearly seen that the pristine sample showed both amorphous and ordered structures. In fact, it is well known that the spin-coated films get trapped in a non-equilibrium structure [6]. In the grazing mode, the pristine and RT rubbed samples gave rise to quite diffuse reflections at 5° and 23°, respectively. But contrarily to what expected, no diffraction features (with the exception of the peak at 5.0° related to the alkyl chain inter-layer distance) were observed for the 70 °C rubbed samples.

Due to the finite resolution of the 2D detector, reflections from well-ordered planes might be lost. Therefore, rotating mode is commonly employed to recover such diffraction features. In fact, as we observe in figure 2(*d*), a better resolved diffraction pattern was obtained in the case of the RT rubbed samples, while similar attempts to refine the signal of the pristine (*a*) and of the 70 °C rubbed film (*c*) were not successful. This represents a further confirmation that an ordered structure is stabilized in the presence of rubbing at RT while no efficient π–π stacking ordering is established during rubbing at 70 °C.

3.3. Optical absorption

In figure 3, we present the normalized absorption spectra of samples rubbed at two different temperatures, namely RT and 70 °C, compared with the pristine sample absorption. The absorption spectra showed three main features: (a) a first shoulder structure at about 596 nm (2.08 eV); (b) a second one at about 549 nm (2.26 eV); (c) a broad feature centred around 515 nm (2.41 eV), which was the maximum of the

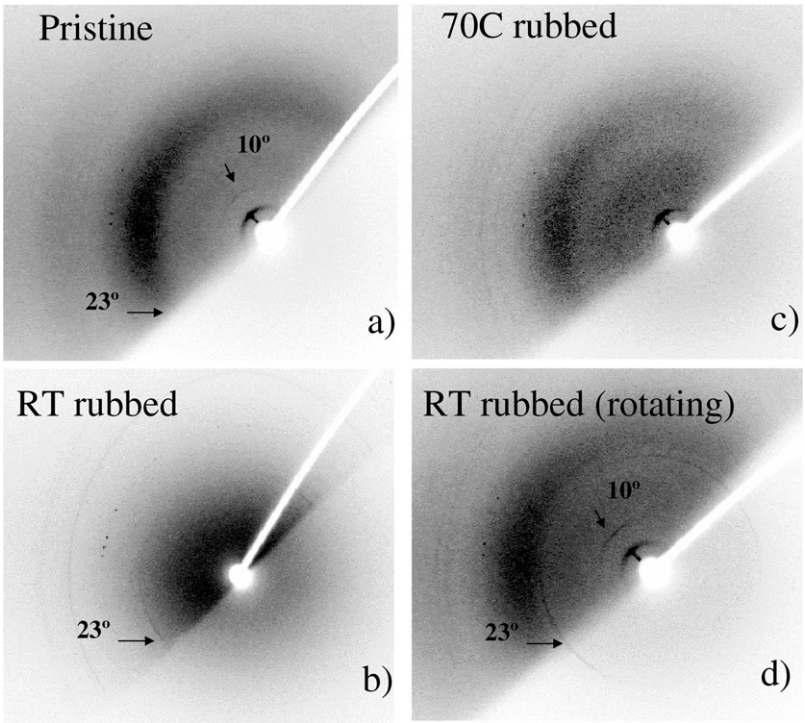

Figure 2. XRD^2 patterns in grazing incidence (1°) of the pristine (*a*), RT rubbed (*b*) and 70 °C rubbed samples (*c*). For the RT rubbed sample the intensity is reported using the rotating mode (*d*).

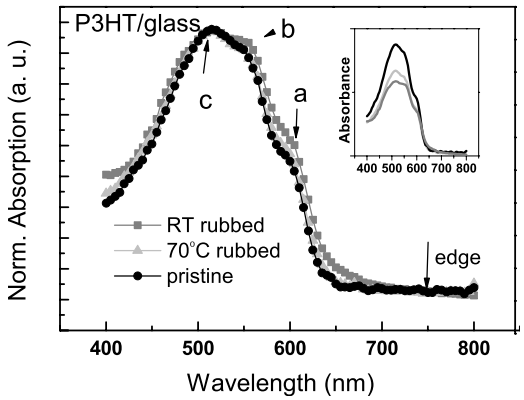

Figure 3. Normalized absorption spectra of the pristine, RT rubbed and 70 °C rubbed P3HT spin-coated films on glass, shown with black, grey and light grey symbols, respectively. In the inset, the absorbance of the three different samples before normalization is reported.

spectrum used for the normalization. In particular, the latter two structures are due to the π–π^* intra-chain transitions of the π conjugated polymer backbone. In contrast, the low energy state at 2.08 eV (a) is not affected by the conjugation length, but is related to inter-chain π–π^* [24] transitions. After rubbing, an intensity increase in the spectral features was observed. Such an effect was more intense for the RT rubbed sample than for the 70 °C rubbed one. These changes, although small because optical absorption was mainly bulk sensitive, were quite appreciable. An increase in the longer wavelength photoabsorption in the RT rubbed sample is clearly evidenced. The exciton energy onset of the absorption is marked by an arrow at 750 nm corresponding to 1.65 ± 0.05 eV.

A vast literature is available on the optical absorption spectra of P3HT. The absorption of solid state films shows remarkable red shift with respect to that of the polymer in solution [25]. When the solid film is formed from a high M_w regio-regular polymer, molecular chains tend to develop from the coil-like structure in solution [26] into more planar, rigid rod-like morphology. Such a morphological change, together with the extended conjugation length in the polymer backbone, induced an extra delocalization of the π states, and consequent decrease in the excitonic energy. In this study, only a limited shift in energy was measured in the case of RT rubbed sample, accompanied by an enhancement in the intensity at 549 nm (b) and at 596 nm (a). These facts suggested an increase in the size of the aligned domains, thus inducing overall enhancement of the overlap between π states both in intra- (b) and inter- (a) chain transitions. Annealing is expected to increase the global crystalline properties even further, however, we have observed a decrease in the features of the 70 °C rubbed sample with respect to the features of the RT rubbed sample.

We suggest that probably annealing played a role in increasing the alignment of the polymer chains but reduced, at the same time, the crystallinity through relaxation effects, as outlined by XRD^2.

By looking at the inset of figure 3, reporting the spectra before normalization, we note that the mechanical rubbing process reduced the optical absorbance in the region of the π–π^* transitions for both RT rubbed and 70 °C rubbed samples. This can be understood in terms of the degree of ordering of the molecules (higher in the RT rubbing case) and the unpolarized status of the light.

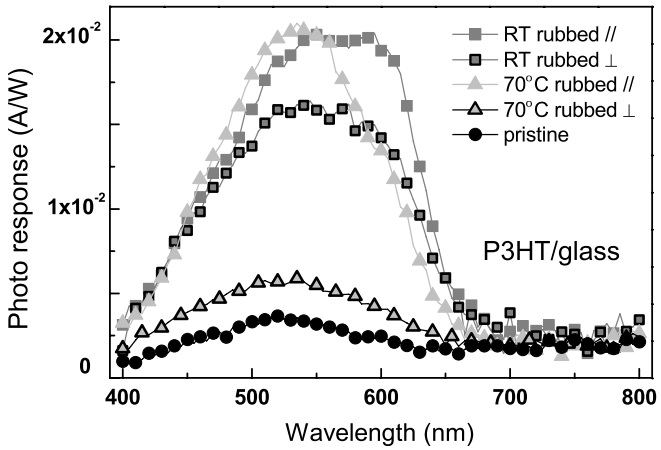

Figure 4. Photoresponse current spectra of pristine, RT rubbed and 70 °C rubbed samples are reported with black, grey and light grey symbols, respectively. Solid symbols are for photocurrents collected between electric contacts parallel (‖) to the rubbing direction, while edged symbols represent the photocurrents taken between electric contacts perpendicular (⊥) to the rubbing direction.

3.4. Photoconductivity

Photoconductivity measured by means of metal contacts on the surface is an appropriate technique to show clear-cut rubbing effects in the recorded photocurrent. It will highlight the results obtained by absorption on the structural changes as well as provide information on the degree of polymer alignment.

Active photoresponse spectra of the samples are reported in figure 4. In all cases, photocurrents were collected by contacts in parallel ('para') and perpendicular ('ortho') configurations with respect to the rubbing direction. In figure 4, photosensitivity of both RT rubbed and 70 °C rubbed samples exhibited significant increase in 'para' spectra (full symbols), if compared with that of the pristine film. In particular the 70 °C rubbed sample attained the largest difference between 'para' and 'ortho' photocurrent. In the latter case the photoconductivity did not deviate considerably from that of the pristine sample. We also observed that the 70 °C rubbed samples had systematically less photoresponse properties than the RT rubbed ones. This lower photosensitivity was related to the lower degree of π–π^* inter-chain interaction already deduced from the absorption spectra (reduced crystallinity). Here a clear confirmation came from the 70 °C rubbed sample in figure 4, with a reduced spectral intensity around 600 nm in the'para' photocurrent related to the inter-chain interaction.

This evidence conjured up a system where an efficient increment of the aligned domains led to faster charge mobility. Thermal annealing induced smaller domain sizes due to relaxation effects with a marked anisotropy in photocurrent, confirming what was previously found by Yang *et al* [20]. After rubbing at 100 °C they observed a relevant dichroic ratio (about 10) of the photocurrent along the rubbing direction under two different polarization conditions of the incident electric field. In contrast, in this study, we observed a striking photoconductivity increase (factor four higher than in the pristine sample) even perpendicularly to the rubbing direction.

In another work from Heil *et al* [19] a strong increase in field effect mobility along the rubbing direction done at 100 °C was obtained. On the other side, the authors found inefficient alignment of highly conductive drop-cast films. The reason was probably that the highly ordered lamellae structures were modified by rubbing at the gate-oxide interface. In this study, where a similar polymer configuration was expected, the rearrangement of the film was not observed by rubbing at 70 °C, even if some hints that disorder increases with temperature have been found.

To summarize the results from photoconductivity confirmed the following picture of the system after rubbing. As well known from studies of the high M_w P3HT films [9], crystalline properties are not directly related to conduction properties. In fact, well-defined boundaries of the film crystalline regions largely limit the mobility [27]. Also in this study, based on figure 2, we can conclude that crystallinity only slightly affects the photoconductivity properties. In fact, we observed that either samples with good planar photoresponse (RT rubbed samples) or weak (pristine samples) had similar crystalline order. In particular, completely disordered XRD patterns were obtained from the 70 °C rubbed films, showing, at least in 'para' configuration, comparably high photocurrent.

3.5. Photoelectron spectroscopy

Photoemission is expected to induce photo-degradation in the polymer films. Actually, changes in the spectra under the Al K_α x-ray source cannot be avoided in these kinds of materials. We nevertheless checked in a dedicated set of samples the chemical composition by fast x-ray measurements. The XPS measurements before and after rubbing (not shown) did not show differences in terms of contaminants, change in the shape and position of the C1s, S2s and S2p core levels, and in terms of increase in the oxygen content. In fact, due to the preparation in air, a normal amount of oxygen was expected. Such contaminants probably reacted with the alkyl chains and did not affect the electronic and optical properties shown above. This result was particularly rewarding in the case of the 70 °C rubbed films. Similar conclusions were also corroborated by comparison with previous experimental data [28] and the results of valence photoemission spectra shown below.

On the other side, no damaging on the samples was observed after UPS measurements on films grown on Si substrates. Here, the very short range sensitivity of UPS spectroscopy was crucial to confirm what was only guessed on the basis of other less surface sensitive techniques.

An oxidation free film, as that in figure 5, shows well-resolved photoemission peaks, namely, a, b, c, d and e . Following the work of Lazzaroni *et al* [29, 30] the peak a can be attributed to the delocalized π states, peak b mainly to the sulfur π states. Peak c and peak d regions are dominated by the alkyl chain σ states (which are not affected by the polymer backbone structural changes), together with the contributions of the aromatic backbone σ states in the c region and localized π states in the d region. Mainly, peak e has C2s character [31, 32]. From the spectrum of the 70 °C rubbed P3HT film, a clear decrease in the delocalized

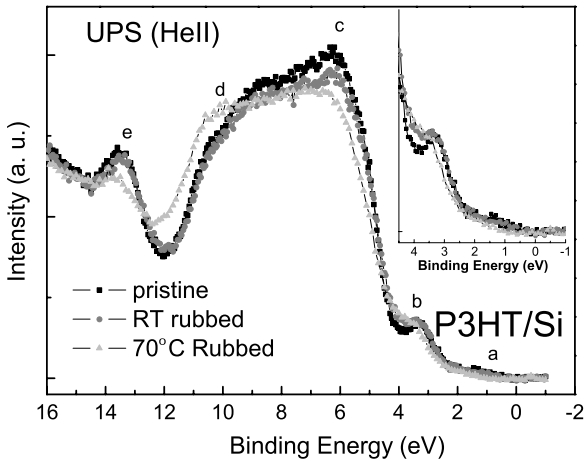

Figure 5. UPS spectra of the pristine (black symbols), RT rubbed (grey symbols) and 70 °C rubbed (light grey symbols) P3HT films measured using He II (40.8 eV) source. Films are on Si substrates with their native oxide. The inset reports in detail the low binding energy region.

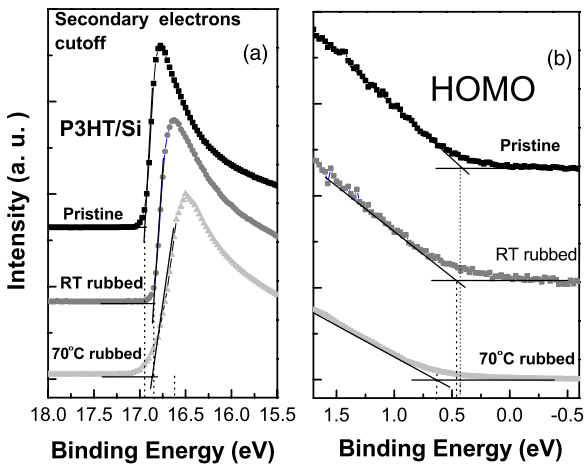

Figure 6. UPS spectra of the pristine, RT rubbed and 70 °C rubbed P3HT films measured using He I source (21.2 eV) with a sample electric bias of −10 V. In (*a*) the secondary cutoff is reported while in (*b*) the HOMO is reported in detail region.

π states (a) and an increase in the localized π density of states (d) were observed with respect to the pristine and RT rubbed films. It confirmed that the annealing treatment introduced the relaxation of the planar chain configuration, resulting in reduced hybridization of the π states along the polymer chain and in the smearing of the features. In the present UPS spectra lower intensity in the region of delocalized π states could not be unambiguously attributed to a planar rearrangement of the molecules. In fact, the geometry of the experiment with the incident photon making an angle of 45° with respect to the sample normal would not efficiently discriminate between the two arrangements.

Highest occupied molecular orbital (HOMO) level and ionization potential of the films can provide further information and a more complete picture of the structural and photo-transport properties of the present system. In the right and left panels of figure 6, we present the UPS spectra obtained by the He I source with a bias of 10 V. In the right panel, the HOMO is reported to determine graphically the highest occupied state. The Fermi energy (zero of the binding energy) was obtained from that of a freshly sputtered metal. Secondary electron cutoffs are shown in the left panel. The ionization potentials of the films were determined by the difference between the photon energy and the energy width from secondary electron cutoff to the HOMO level [33]. HOMO energy of the 70 °C rubbed film was 0.63 eV, while the RT rubbed and pristine films had similar values of 0.41 eV and 0.42 eV, respectively. The higher energy of the HOMO value was expected in response to the reduction in the delocalized π states in the 70 °C rubbed film. The 70 °C rubbed film also showed the highest ionization potential of 5.01 eV, when RT rubbed and pristine samples had equivalent ionization potential values of 4.8 eV and 4.69 eV, respectively. From the energy point of view the above measurements indicated that rubbing and temperature both relaxed the polymer chains to a more stable state.

4. Discussion and conclusions

High M_w regio-regular P3HT films are composed of crystalline domains within an amorphous matrix. The two-dimensional conductivity of the film is due to the efficient interconnection of crystalline domains where packing of chains occurs [9]. Photoconductivity in P3HT films is then governed by the fastest charge carrier mobility along the polymer chains, with intra-chain hopping between portions of conjugated segments of the polymer, but limited by the slower (inter-chain) hopping mobility between stacking planes along rod-like structures [2]. The rubbing process, done at RT, induced an overall ordering of the film as recorded by the XRD. An increase in the conductivity in both the 'para' and 'ortho' directions is the consequence of the ordering. The crystalline portion of the film will be connected coherently by long polymer chains along the rubbing direction, while along the 'ortho' direction the stacking planes contribute to an isotropic photoconductivity.

When rubbing is performed at higher temperatures, a sizeable increase in the long polymer chains is accompanied by a corresponding deformation of the crystalline region, with a sudden increase in the dimension of the disordered regions between ordered packets of molecules. As shown by the present AFM images, heating during rubbing induced an important structural deformation in the sample, whose main consequence was the decrease in the inter-chain interaction and the related hopping charge transfer. This can be observed from the response spectrum of the photocurrent parallel to the rubbing direction (figure 4), where the shoulder feature associated with the inter-chain interaction was notably quenched.

In summary, when compared with the 70 °C rubbed and the pristine samples, a better local order arrangement of the RT rubbed P3HT films was deduced from the absorption spectra and XRD, showing slight red shift and more intense features. In this case, highly isotropic photoconductivity was obtained as a combined effect of alignment of chains and inter-chain hopping between well-ordered lamellae.

Samples rubbed at 70 °C showed a morphological rearrangement, being at the origin of a remarkable anisotropy

of photoconductivity along the rubbing direction. Such an anisotropy was related to a better global order, in terms of alignment of the polymer chains, but was accompanied by a strong relaxation of the crystalline components and by quenching of inter-chain interactions. Valence band photoemission confirmed these structural characteristics, indicating higher ionization potential and deeper HOMO levels, for the 70 °C rubbed films, corroborating the present picture.

References

[1] Sirringhaus H *et al* 1999 *Nature* **401** 685
[2] Salleo A 2007 *Mater. Today* **10** 38 and references therein
[3] Salleo A, Chabinyc M L, Yang M S and Street R A 2002 *Appl. Phys. Lett.* **81** 4383
[4] Shaheen S E, Brabec C J, Sariciftci N S, Padinger F, Fromherz T and Hummelen J C 2001 *Appl. Phys. Lett.* **78** 841
[5] Reyes-Reyes M, Kim K and Carroll D L 2005 *Appl. Phys. Lett.* **87** 083506
[6] Hugger S, Thomann R, Heinzel T and Thurn-Albrecht T 2004 *Colloid Polym. Sci.* **282** 932
[7] Kim D H, Han J T, Park Y D, Jang Y, Cho J H, Hwang M and Cho K 2006 *Adv. Mater.* **18** 719
[8] Kline R J, McGehee M D, Kadnikova E N, Liu J S, Frechet J M J and Toney M F 2005 *Macromolecules* **38** 3312
[9] Kline R J, McGehee M D, Kadnikova E N, Liu J S and Frechet J M J 2003 *Adv. Mater.* **15** 1519
[10] Zhang R *et al* 2006 *J. Am. Chem. Soc.* **128** 3480
[11] Sirringhaus H, Tessler N and Friend R H 1998 *Science* **280** 1741
[12] Zen A *et al* 2006 *Macromolecules* **39** 2162
[13] Brinkmann M and Rannou P 2007 *Adv. Funct. Mater.* **17** 101
[14] Grell M and Bradley D D C 1999 *Adv. Mater.* **11** 895
[15] Toney M F, Russell T P, Logan J A, Kikuchi H, Sands J M and Kumar S K 1995 *Nature* **374** 709
[16] Mardalen J, Samuelsen E J, Gautun O R and Carlsen P H 1992 *Synth. Met.* **48** 363
[17] Derue G, Coppee S, Gabriele S, Surin M, Geskin V, Monteverde F, Leclere P, Lazzaroni R and Damman P 2005 *J. Am. Chem. Soc.* **127** 8018
[18] Bolognesi A *et al* 2004 *Polymer* **45** 4133
[19] Heil H, Finnberg T, von Malm N, Schmechel R and von Seggern H 2003 *J. Appl. Phys.* **93** 1636
[20] Yang C Y, Soci C, Moses D and Heeger A J 2005 *Synth. Met.* **155** 639
[21] Sirringhaus H, Tessler N and Friend R H 1999 *Synth. Met.* **102** 857
[22] Horcas I, Fernandez R, Gomez-Rodriguez J M, Colchero J, Gomez-Herrero J and Baro A M 2007 *Rev. Sci. Instrum.* **78** 013705
[23] Prosa T J, Winokur M J, Moulton J, Smith P and Heeger A J 1992 *Macromolecules* **25** 4364
[24] Brown P J, Thomas D S, Kohler A, Wilson J S, Kim J S, Ramsdale C M, Sirringhaus H and Friend R H 2003 *Phys. Rev.* B **67** 064203
[25] Patil A O, Heeger A J and Wudl F 1988 *Chem. Rev.* **88** 183
[26] Neher D 1995 *Adv. Mater.* **7** 691
[27] Horowitz G, Hajlaoui M E and Hajlaoui R 2000 *J. Appl. Phys.* **87** 4456
[28] Shimomura A, Ikejima Y, Yajima K, Yagi T, Goto T, Gunnella R, Abukawa T, Fukuda Y and Kono S 2004 *Appl. Surf. Sci.* **237** 75
[29] Lazzaroni R, Sato N, Salaneck W R, Dossantos M C, Bredas J L, Tooze B and Clark D T 1990 *Chem. Phys. Lett.* **175** 175
[30] Ghijsen J, Lazzaroni R, Parente V, Bredas J L, Lachkar A, Selmani A and Johnson R L 1996 *J. Electron Spectrosc. Relat. Phenom.* **78** 355
[31] Salaneck W R, Inganäs O, Thémans B, Nilsson J O, Sjögren B, Österholm J E, Brédas J L and Svensson S 1988 *J. Chem. Phys.* **89** 4613
[32] Chua L L, Dipankar M, Sivaramakrishnan S, Gao X Y, Qi D C, Wee A T S and Ho P K H 2006 *Langmuir* **22** 8587
[33] Knupfer M and Peisert H 2004 *Phys. Status Solidi* A **201** 1055